A comparison between conventional photothermal frequency scan and the lock-in rate window method in measuring thermal diffusivity of solids

Mahendra Munidasa and Andreas Mandelis
Photothermal and Optoelectronic Diagnostics Laboratory, Department of Mechanical Engineering and Manufacturing Research Corporation of Ontario, University of Toronto, 5 King's College Road, Toronto, Ontario, Canada M5S 1A4

(Received 21 December 1993; accepted for publication 24 March 1994)

A comparison between the conventional photothermal frequency scan method and the recently developed photothermal lock-in rate window technique for thermal diffusivity measurements of materials, is presented. In this comparison, a completely noncontact experimental configuration has been utilized based on infrared photothermal radiometry. This work shows that for thick materials with long thermal transport times across the sample where low-frequency measurements are required, the frequency scan method may be more appropriate due to its simplicity. The rate window method, however, gives superior signal-to-noise ratio (SNR) for materials with very short thermal transport times such as metal foils, which otherwise require high frequency, low SNR measurements. A further advantage of the pulse duration-scanned rate-window mode is that it does not require knowledge of the instrumental transfer function as an input.

I. INTRODUCTION

Several experimental techniques have been developed to measure thermal conductivity of materials by steady-state heat flow methods and thermal diffusivity by dynamic (time-dependent) heat flow methods. The thermal diffusivity α is related to the conductivity k by

$$\alpha = \frac{k}{\rho c}, \tag{1}$$

where ρ is the density and c is the specific heat capacity of the material. The product, ρc is the thermal capacitance per unit volume which is not expected to change much for different types of solids of the same family (e.g., different kinds of steel[1]), or due to some engineering processes such as surface hardening.[2] Thus by measuring thermal diffusivity one can compute the thermal conductivity by using the tabulated value of ρc. Therefore, dynamic methods which allow faster measurements of thermal diffusivity are characterized by their relative insensitivity to background fluctuations and boundary losses,[3] and have increasingly become more popular than the steady-state conductivity measurements.

Thermal diffusivity itself is a thermophysical parameter which gives both direct and indirect information on materials of industrial interest. The direct knowledge of thermal diffusivity is required, for example, for modeling of cooling and heating of machinery, or heat resistant coatings, heat sinks or spreaders. Indirect information provided by thermal analysis is also a powerful tool, for example, in the curing of reaction-molding resins,[4] the nondestructive depth profiling of surface modified metals,[5] and potentially in the *in situ* quality control of manufactured metal sheets, which is the ultimate goal of the present work.

There exist two basic types of time-dependent methods to measure thermal diffusivity: (1) the periodic heat flow method[6] and (2) transient methods.[7,8] In the former method, a sample of known thickness is irradiated with a harmonically modulated laser beam launching a thermal wave, and the periodic temperature at the front or the back surface of the sample is monitored at several modulation frequencies f (frequency-scan method). The frequency-dependent thermal diffusion length μ given by

$$\mu = \sqrt{\frac{\alpha}{\pi f}} \tag{2}$$

is related to the phase lag of the detected temperature wave with respect to the heating source which may be monitored using a lock-in amplifier. In transient methodologies, such as pulsed[7] or multifrequency spectral excitation,[8] a sample of known thickness is irradiated on one side with a laser pulse; then the time evolution of the temperature on either side is monitored and the rate of decay is related to the diffusivity. In a recent development, pulse heating has been combined with lock-in detection (lock-in rate window)[9] to obtain transient-equivalent data with superior signal-to-noise ratio to the conventional pulse averaging. This technique has evolved from the deep-level-transient spectroscopic (DLTS) measurement techniques[10] in semiconductor research. In this paper, we will compare the lock-in rate window method with the periodic heating method, since they are closely related with respect to lock-in noise filtering.

II. EXPERIMENT

In this work, we used a large heating beam radius so that the heat flow is one dimensional. Both heating and temperature monitoring was done on the same side of the sample. Therefore, the sample has to be thin enough (and of known thickness) such that the front surface temperature is affected by the back boundary. The temperature was monitored in a noncontact manner by measuring the IR radiation emitted from the sample surface. A complete description of the infrared radiometric experimental configuration can be found elsewhere.[5] A digital lock-in amplifier (Stanford Research

 0034-6748/94/65(7)/2344/7/$6.00

System, model SR850) was used to measure the photothermal signal. The analog-to-digital converter (ADC) in the Lab Master DMA (Scientific Solutions, Inc.) was employed to read the analog output of the lock-in by the computer. Pulses for the acousto-optic (A/O) modulator to modulate the laser beam intensity pulse profile and frequency/repetition rate (which was also used as the reference signal for the lock-in) were generated by programming the 9513A system timing controller output on the Lab Master DMA motherboard. The power density used (at 50% duty cycle) was the same for all the measurements described below. It was necessary to allow the system to come to thermal equilibrium, with the laser on, so that the unmodulated temperature of the sample reached steady state, before collecting data.

A. Frequency-scan method

A one-dimensional analysis of the diffusion and reflection of the thermal wave generated by a laser beam modulated at angular frequency ω, yields the following expression for the ac temperature at the irradiated surface:[3]

$$T(\omega)=\frac{I_0\eta_s}{k_s\sigma_s(1+b_{gs})}\cdot\frac{1+R_{gs}\exp(-2\sigma_s L)}{1-R_{gs}^2\exp(-2\sigma_s L)}, \tag{3}$$

where L is the thickness and k_s is the thermal conductivity of the sample; I_0 is the laser irradiance; η_s is the optical-to-thermal energy conversion efficiency at the sample surface; and b_{gs} is the thermal coupling coefficient to the surrounding gas (air) given by

$$b_{gs}=\frac{k_g/\sqrt{\alpha_g}}{k_s/\sqrt{\alpha_s}}. \tag{4}$$

Here, k_j is the thermal conductivity and α_j is the thermal diffusivity of medium (j) with the subscripts s and g referring to the sample and the gas, respectively. The quantity R_{gs} given by

$$R_{gs}=\frac{1-b_{gs}}{1+b_{gs}} \tag{5}$$

is the thermal-wave reflection coefficient at the solid–gas interface and σ_s is a complex diffusion coefficient given by

$$\sigma_s=(1+i)\sqrt{\frac{2\alpha_s}{\omega}}. \tag{6}$$

It is assumed that the solid and air are in perfect thermal contact. Expressions for the measured quantities, phase and magnitude, can be derived from the real and imaginary parts of Eq. (3). The measurements are made with respect to a thermally thick ($L\gg\mu$) reference sample where the signal is given by

$$T_{\rm ref}(\omega)=\frac{I_0\eta_r}{k_r\sigma_r(1+b_{gr})}, \tag{7}$$

to compensate for the instrumental transfer function. For radiometric detection both $T(\omega)$ and $T_{\rm ref}(\omega)$ expressions must be multiplied by terms including surface emissivity, detector parameters, ambient temperature, etc.[5] This constant multiplicative term, except for the sample-dependent terms, is cancelled out from the normalized signal [Eq. (3) divided by Eq. (7)].

By fitting the normalized experimental data (phase and magnitude) frequency dependence to the corresponding expressions derived from Eq. (3), the parameters R_{gs} and $L/(\alpha_s)^{1/2}$ can be calculated. Since the coupling medium is air ($k_g=0.026$ W m^{-1} K^{-1}, $\alpha_g=3.1\times10^{-5}$ m^2 s^{-1}),[3] the value of $b_{gs}\ll1$. Therefore, R_{gs} is almost unity and its sensitivity to k_s is extremely small. That simplification makes $L/(\alpha_s)^{1/2}$ to be the only fitting parameter for normalized phase data. In addition to $L/(\alpha_s)^{1/2}$ the normalized amplitude data contain a multiplicative factor due to any differences in the bulk thermal properties and the surface finish between the sample and the reference. This factor may be cancelled out by setting the amplitude ratio to be unity at the high-frequency (thermally thick) end where the phase difference is expected to be zero.[11] Setting the amplitude ratio equal to unity is possible because we are only interested in the shape of the normalized curve, not in the absolute magnitude. Since there exists an extremum in the frequency curve of both magnitude and phase which is very sensitive to $L/(\alpha_s)^{1/2}$, it is not necessary to fit an entire frequency range. This could be used as a fast on-line measurement of small variations in L or α_s in an industrial environment. Experimental frequency-scan data (3 to 155 Hz) from a 440 μm thick stainless steel type 304 sample and the corresponding theoretical fit to Eq. (3) are shown in Fig. 1. The best fit was found to occur for a thermal diffusivity of 4.8×10^{-6} m^2 s^{-1}. Two other curves corresponding to α_s of 3.95×10^{-6} and 5.5×10^{-6} m^2 s^{-1} are also shown in order to assess the sensitivity of the fit to the absolute value of the diffusivity. Figure 2 shows similar data from a foil of thickness 25.4 μm from an unknown metallic material within a frequency range of 10–100 kHz. These data exhibit severe scatter around the extremum and are therefore difficult to fit to the theoretical expression, Eq. (3) with any reasonable degree of accuracy. The theoretical curves correspond to diffusivities of $1.15\times10\times10^{-5}$, 1.31×10^{-5}, and 1.03×10^{-5} m^2 s^{-1}. The experimental results in Fig. 2 are optimized in the sense that digital lock-in outputs exhibit superior signal-to-noise ratios to conventional analog lock-ins.[12] Yet, the combination of the large scatter observed throughout the measurement frequency range *and* the relative insensitivity of the theoretical curves to the actual value of α_s for deviations of this parameter up to 40%, and, perhaps, higher, unfortunately leads to the conclusion that frequency-scanned photothermal radiometry is not easily applicable to thin metallic layers.

B. The lock-in rate window method

In this method[9,13] the sample is irradiated with a repetitive square laser pulse of duration τ_p and period T_0. The evolution of temperature in the sample is governed by the thermal diffusion equation.[9] Solving this equation in the Laplace domain with appropriate boundary conditions and transforming to the time domain, one can obtain the temperature evolution $T_R(t)$ at the irradiated surface given by

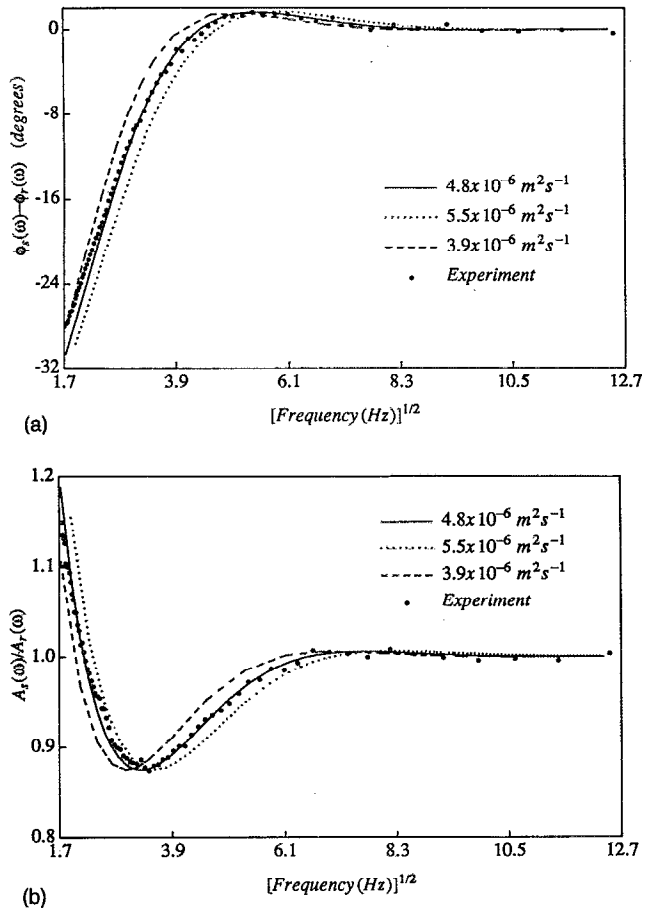

FIG. 1. Experimental (filled circles) frequency-scanned (a) phase data and (b) amplitude data, for a 440 μm thick steel plate normalized to a semi-infinite reference sample and the corresponding theoretical curves for thermal diffusivities of 4.8×10^{-6} (solid), 5.5×10^{-6} (dots), and 3.9×10^{-6} (dashes) $m^2\,s^{-1}$.

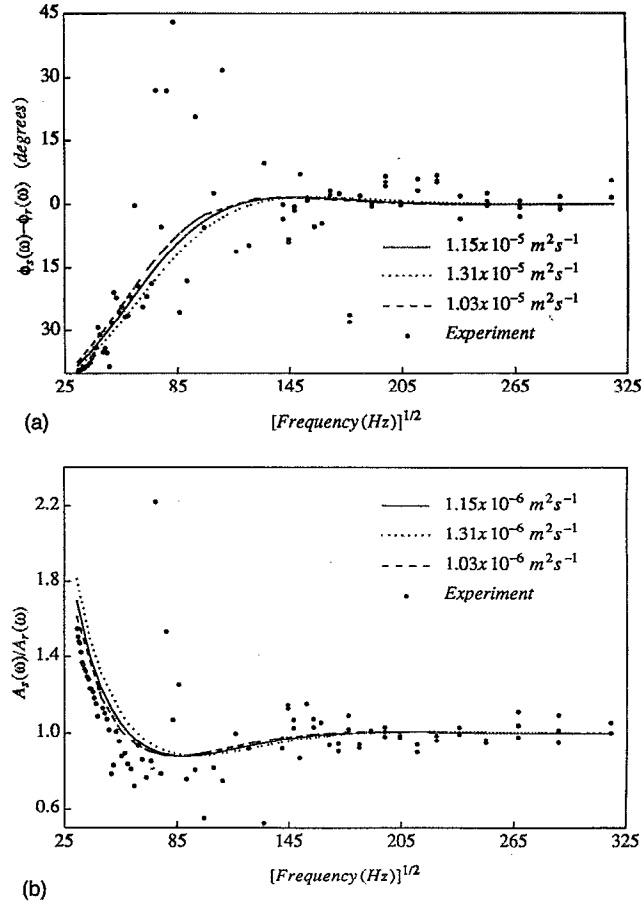

FIG. 2. Experimental (filled circles) frequency-scanned (a) phase data and (b) amplitude data, for a 25.4 μm thick metal foil, normalized to a semi-infinite reference sample and the corresponding theoretical curves for thermal diffusivities of 1.15×10^{-5} (solid), 1.31×10^{-5} (dots), and 1.03×10^{-5} (dashes) $m^2\,s^{-1}$.

$$T_R(t)=\begin{cases}F_R(t); & t\leqslant\tau_p\\ F_R(t)-F_R(t-\tau_p); & T_0\geqslant t\geqslant\tau_p\end{cases}, \tag{8}$$

where

$$F_R(t)=K\sqrt{t}\sum_{n=0}^{\infty}\left\{R_{gs}^{2n+1}\ i\mathrm{erfc}\left[\frac{(n+1)L}{\sqrt{\alpha_s t}}\right]+R_{gs}^{2n}\ i\mathrm{erfc}\left[\frac{nL}{\sqrt{\alpha_s t}}\right]\right\}. \tag{9}$$

Here, K is a constant independent of the characteristic thermal time constant L^2/α_s and the function $i\mathrm{erfc}(x)$ is defined as

$$i\mathrm{erfc}(x)=\frac{1}{\sqrt{\pi}}e^{-X^2}-x\ \mathrm{erfc}(x)\ , \tag{10a}$$

where

$$\mathrm{erfc}(x)=\frac{2}{\sqrt{\pi}}\int_x^{\infty}e^{-y^2}\,dy. \tag{10b}$$

Since this is a repetitive heating process, it is necessary to take into consideration, the effect of earlier pulses. A rigorous calculation which involves solving of the diffusion equation with periodic boundary conditions shows that a simple linear superposition during any pulse interval,

$$S_R(t)=\begin{cases}F_R(t)+\sum_{k=1}^{\infty}[F_R(t+kT_0)-F_R(t-\tau_p+kT_0)]; & t\leqslant\tau_p\\ \sum_{k=0}^{\infty}[F_R(t+kT_0)-F_R(t-\tau_p+kT_0)]; & T_0\geqslant t\geqslant\tau_p\end{cases} \tag{11}$$

is valid.

In the lock-in rate-window method, $S_R(t)$ is the input to the lock-in amplifier with a reference signal of frequency $1/T_0$. This method has the advantage of combining the superior signal-to-noise ratio of a tuned electronic filter, used in the frequency domain detection, with the simple and straightforward interpretation of the time-domain photothermal signal $S_R(t)$. The lock-in measures the fundamental Fourier component of $S_R(t)$ with an amplitude c_1 and phase ϕ_1 given by

$$c_1=(a_1^2+b_1^2)^{1/2},\quad \phi_1=\tan^{-1}(b_1/a_1), \tag{12}$$

where

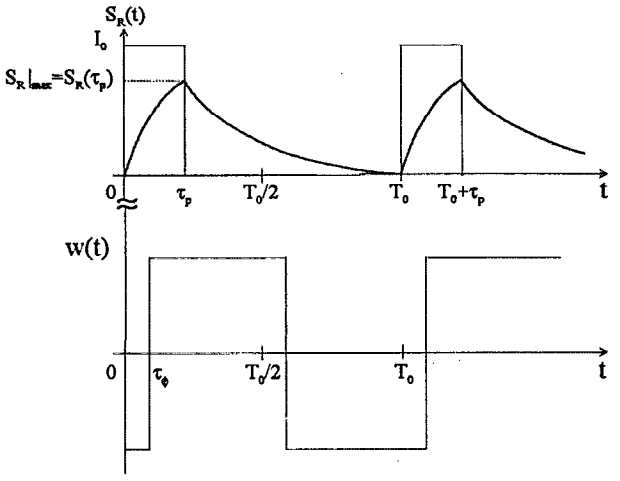

FIG. 3. Photothermal repetitive transient signal $S_R(t)$ due to a pulse of duration τ_p and period T_0. The lock-in weighing function $w(t)$ is also shown with the same period and a phase delay τ_ϕ.

$$a_1(T_0)=\frac{2}{T_0}\int_0^{T_0} S_R(t)\cos(\omega_0 t)dt,$$
$$b_1(T_0)=\frac{2}{T_0}\int_0^{T_0} S_R(t)\sin(\omega_0 t)dt, \tag{13}$$

and

$$\omega_0=\frac{2\pi}{T_0}. \tag{14}$$

Now, the in-phase and quadrature components of the lock-in output are obtained by weighing both the corresponding fundamental Fourier components,

$$f_I(t)=c_1\cos(\omega_0 t+\phi_1) \tag{15}$$

and

$$f_Q(t)=c_1\sin(\omega_0 t+\phi_1), \tag{16}$$

by the square-wave lock-in reference function $w(t)$ of duration T_0. At this point, we will take into consideration any frequency-dependent instrumental phase shifts by including a time shift $\tau_\phi(T_0)$ into the reference as shown in Fig. 3. The result of this operation under long lock-in filter time constant is

$$S_I(T_0)=\frac{1}{T_0}\int_0^{T_0} f_I(t)w(t)dt$$
$$=\frac{1}{T_0}\left[-\int_0^{\tau_\phi(T_0)} f_I(t)dt+\int_{\tau_\phi(T_0)}^{T_0/2+\tau_\phi(T_0)} f_I(t)dt\right.$$
$$\left.-\int_{T_0/2+\tau_\phi(T_0)}^{T_0} f_I(t)dt\right]$$
$$=\frac{2c_1}{\pi}\sin[\omega_0\tau_\phi(T_0)+\phi_1(T_0)] \tag{17}$$

and similarly

$$S_Q(T_0)=-\frac{2c_1}{\pi}\cos[\omega_0\tau_\phi(T_0)+\phi_1(T_0)]. \tag{18}$$

If the lock-in reference phase is tuned for all T_0 so as to align the positive edge of the reference square-wave with the rising edge of the optical pulse, $\tau_\phi(T_0)$ will be zero and the lock-in output signals will be

$$S_I(T_0)=\frac{2b_1(T_0)}{\pi} \tag{19}$$

and

$$S_Q(T_0)=-\frac{2a_1(T_0)}{\pi}. \tag{20}$$

Calculations show that the quadrature of the lock-in signal saturates (i.e., reaches a particular value which remains unchanged thereafter) after a superposition of about ten pulses in the time-domain photothermal signal $S_R(t)$ [Eq. (11)] and it agrees with the experimental data, whereas it is computationally very difficult for the in-phase component to saturate. This is probably due to the fact that the cosine weighing function will tend to emphasize the initial part of the decay transient, while the sine weighing function tends to emphasize the later part.[14]

In the photothermal lock-in rate-window method, the scanning of the rate window is performed either by changing the period T_0 of the repetitive heating pulse with constant pulse duration τ_p, or by changing pulse duration at a fixed period.

Cancelling out the instrumental frequency dependence is not straightforward in this technique as in the frequency-scan method. Our experience shows that most of the instrumental effects come from the frequency-dependent phase of the lock-in amplifier, especially below 30 Hz and above 10 kHz (models SR850 and EG&G model 5210). In the case of rate-window T_0 scan, it is possible to find the function, $\tau_\phi(T_0)$, from a polynomial fit to a frequency-scan phase data from a homogeneous semi-infinite reference sample. In the case of pulse duration scan, the lock-in phase can be tuned manually so that the phase of the signal from a homogeneous semi-infinite reference sample at frequency $1/T_0$ (50% duty cycle) is $-45°$ as expected theoretically from Eq. (3) in the limit $L\to\infty$ [i.e., Eq. (7)], before taking rate-window data. This makes scanning the pulse duration more convenient because there is no change in the instrumental transfer function, which only depends on the T_0. Nevertheless, this method has a resolution disadvantage with regard to the position of the quadrature minimum, as will be seen below. Experimental quadrature signal data from a rate-window scan by scanning the period from 51 to 130 ms with a pulse duration of 50 ms, and the corresponding theoretical fit $S_Q(T_0)$ for the same stainless steel sample described earlier are shown in Fig. 4. The three theoretical curves correspond to the same thermal diffusivities used to calculate frequency scan data in Fig. 1 and the best fit is entirely consistent with the frequency scan data. These data were taken with the lock-in phase tuned to a semi-infinite reference sample at 100 ms (10 Hz), which is the 50% duty cycle point. The minimum occurs around that point, and the theoretical curves were calculated using Eq.

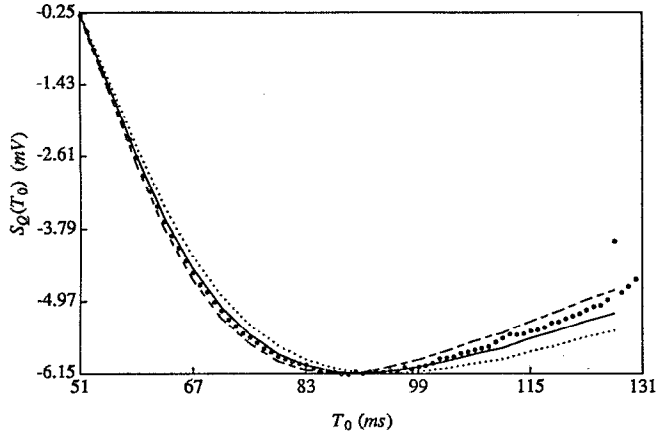

FIG. 4. Experimental quadrature data (filled circles) from a rate-window T_0 scan for the 440 μm steel plate of Fig. 1 and the theoretical curves (normalized to the experimental minimum) corresponding to diffusivities of 4.8 (solid), 5.5 (dots), and 3.9 (dashes)$\times 10^{-6}$ m^2 s^{-1}.

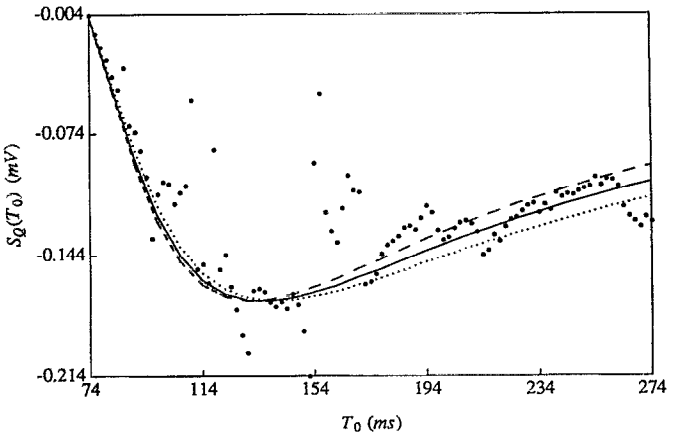

FIG. 6. Experimental quadrature data (filled circles) from a rate-window T_0 scan for the 25.4 μm thick metal foil of Fig. 2 and the theoretical curves (normalized to the experimental minimum) corresponding to diffusivities of 1.15 (solid), 1.31 (dots), and 1.03 (dashes)$\times 10^{-5}$ m^2 s^{-1}.

(20). The discrepancy between the data and the theory at longer periods may be due to the lack of adequate compensation for the instrumental effects. It is interesting to note that an analogous divergence of the frequency-scanned phase data from the theoretical fit in Fig. 1(a) is also evident in the low-frequency regime of that figure. The quality (SNR) of this rate-window data and the resolution of the extremum are comparable to the frequency-scan data of Fig. 1. Figure 5 shows the experimental quadrature data from a rate-window scan at a fixed period of 100 ms and a variable pulse duration (1–99 ms) for the same sample. Again, the best fit corresponds to a diffusivity of 4.8×10^{-6} m^2 s^{-1}, but no discrepancies between data and theory are evident anywhere in the scanned time range. Here, the reference phase was adjusted at 10 Hz (100 ms, which is the scan period used) such that the signal phase from a semi-infinite reference sample was $-45°$ and was valid for all the data points providing an excellent fit. Unfortunately, the sensitivity of the position of the second extremum (minimum) to the variations in the diffusivity is extremely poor. Therefore, it was found necessary to fit the whole curve.

Rate-window scan data at a fixed pulse duration of 73 μs from the metal foil of thickness 25.4 μm described earlier are shown in Fig. 6. The lock-in phase was adjusted at 6.849 kHz (146 μs), which is the 50% duty cycle point. The instrumental frequency dependence of the phase was relatively flat in the frequency range of these data. The range of diffusivities (1.31×10^{-5}–1.03×10^{-5} m^2 s^{-1}) that could be reasonably fitted, with a median value (solid line) of 1.15×10^{-5} m^2 s^{-1} is also shown in Fig. 6. Note that the same values were used to calculate the theoretical curves in Fig. 2, however, it is clear that the possible range of diffusivities for the frequency-scan data is much wider owing to their poorer SNR, the absence of pronounced extrema in both amplitude and phase data, and the wide disagreement between normalized amplitude data and the theoretical curves around the minimum of Fig. 2(b). The corresponding rate-window pulse duration scan at a fixed period of 146 μs is shown in Fig. 7.

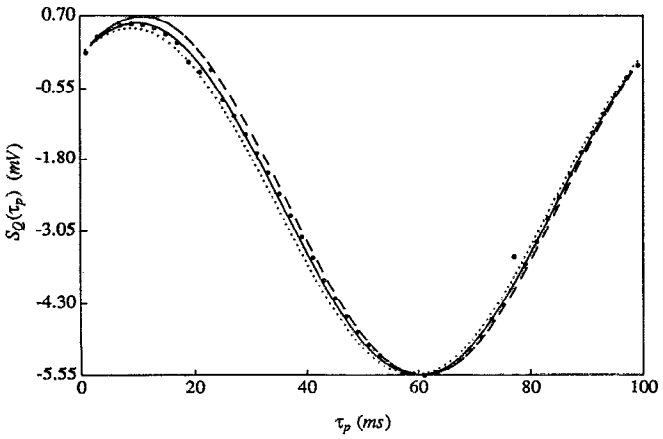

FIG. 5. Experimental quadrature data (filled circles) from a rate-window τ_p scan for the 440 μm steel plate of Fig. 1 and the theoretical curves (normalized to the experimental minimum) corresponding to diffusivities of 4.8 (solid), 5.5 (dots), and 3.9 (dashes)$\times 10^{-6}$ m^2 s^{-1}.

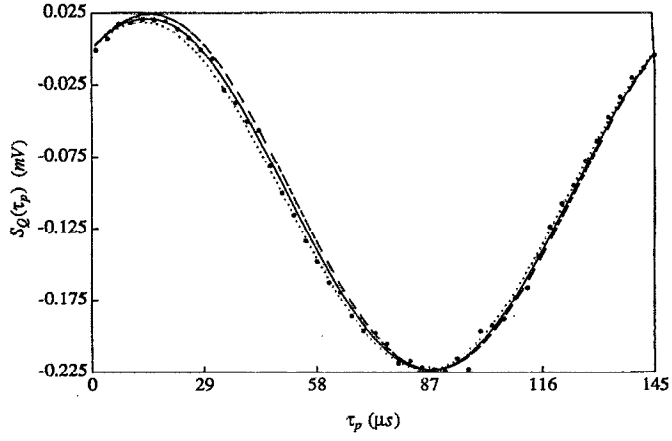

FIG. 7. Experimental quadrature data (filled circles) from a rate-window τ_p scan for the 25.4 μm thick metal foil of Fig. 2 and the theoretical curves (normalized to the experimental minimum) corresponding to diffusivities of 1.15 (solid), 1.31 (dots), and 1.03 (dashes)$\times 10^{-5}$ m^2 s^{-1}.

This clearly shows a much better signal-to-noise ratio than either Fig. 6 or 2, with the tolerance in the acceptable α_s values being less than 13%.

III. DISCUSSION

In this paper, we have compared experimentally two photothermal techniques capable of measuring thermal diffusivities of solid samples of finite thickness. Here, we have considered two different samples, one with long thermal transport time L^2/α_s where low-frequency measurements are required and another sample with short thermal transport time where high-frequency measurements are required. For high-frequency measurements, due to the drop in the photothermal signal amplitude, there is a considerable decrease in the signal-to-noise ratio for a given laser irradiance. We have shown that the conventional frequency scan method may be a better choice at low frequencies because of the simple experimental procedure and the straightforward analytical calculations using simple expressions, although the SNR and sensitivity to the absolute α_s value is comparable to the repetition period-scanned rate-window method [see Figs. 1(a) and 4]. Lock-in rate-window calculations involve more complicated expressions where several numerical solutions are required. These sometimes can introduce errors.

At high frequencies, however, the pulse-duration scanned lock-in rate-window technique gives signal-to-noise ratio superior to both frequency-scanned detection and repetition period-scanned rate-window detection, as seen from Figs. 2, 6, and 7. This rate-window technique requires a theoretical fit to the data over a significant range of pulse durations to determine the best-fit value of the thermal diffusivity, owing to the lack of positional resolution of the curve extrema. Excellent fits are possible resulting in α_s value determinations in thermally thin samples much better than the uncertainty limits of $\pm 13\%$ shown in Fig. 7. By comparison, using the same instrumentation and thin foil sample, the repetition period-scanned rate-window technique gave the value of α_s with uncertainty in the range of $\pm 13\%$, Fig. 6, due to the degraded SNR. Here, a theoretical fit to the *entire* T_0 scanned range is necessary, while its potential advantage of higher minimum positional resolution that a τ_p scan is of little relevance because of the increased noise. In addition, the instrumental transfer function can be cancelled out conveniently in the τ_p scan. Finally, the conventional frequency-scanned method is by far the worst, exhibiting extremely degraded SNR resulting in unacceptable high uncertainties in the measurement of α_s values. In fact, the theoretical curves in Fig. 2 corresponding to thin metal foil diffusivity values of $1.03-1.31\times10^{-5}$ $m^2\,s^{-1}$ were drawn after the best-fit value was estimated in Fig. 7. Otherwise, there would be no possible estimate of the most probable α_s value in the presence of the high noise levels of Fig. 2.

In agreement with detailed theoretical considerations of the SNR advantage of the τ_p- or T_0-scanned rate-window method over the frequency-scanned approach,[15] it is clear that the transient nature of the rate-window signal is responsible for it. Qualitatively, the lock-in amplifier captures the first Fourier coefficient of the photothermal transient in the former case; in the latter case, it monitors the fundamental Fourier coefficient of the harmonic photothermal signal. It is well known from time- and frequency-domain analyses of photothermal signals[16] that in the thermal transient the optically imparted energy distributes itself in such a manner that it provides the strongest response at times immediately following the pulse cutoff. This is, precisely, the range of scanned times involved in the rate-window technique which therefore yields a strong fundamental coefficient magnitude of the Fourier series representation of the repetitive pulse. Conversely, in harmonic photothermal analysis the fundamental Fourier coefficient of the repetitive 50% duty cycle pulse decreases in magnitude in inverse proportion to the strength of the first Fourier coefficient of the time-domain pulse, due to the inverse relationship between time- and frequency-domain and the Parseval theorem.[17] Therefore, fast photothermal phenomena are expected to yield fundamental Fourier coefficients of superior strength in the transient repetitive pulse mode to the one allotted to the respective high-frequency fundamental component under harmonic excitation, and the higher the frequency, the higher the strength contrast of the fundamentals in the two transform domains. The result is, of course, higher SNR for the transient response (commonly observed as the strong early time response of pulsed laser photothermal systems[7]). A more detailed theoretical analysis of the foregoing qualitative remarks is currently underway.

It should be kept in mind that in this one-dimensional, single-ended, backscattered photothermal approach it is necessary to choose the right frequency (or repetition period) range such that the sample is thermally thin, in order to determine the diffusivity of the material. In the frequency scan method, it is the range where the extremum occurs. In the rate-window method the right range is not so obvious from the in-phase or quadrature data. It is therefore necessary to check the signal phase at the 50% duty cycle point to ascertain thermal thinness, using as the criterion the deviation from the semi-infinite reference sample signal phase $(-45°)$.[11]

It is possible to use a focused laser beam and monitor the temperature away from the heated spot on the same surface where three-dimensional heat flow has to be taken into consideration. In this case, the sample may be of any thickness which does not have to be known but the theoretical analysis is less straightforward.

ACKNOWLEDGMENT

The support of the Manufacturing Research Corporation of Ontario (MRCO) is gratefully acknowledged.

[1] *Metals Handbook, Desk Edition*, edited by H. E. Boyer and T. L. Gall (American Society of Metals, Metals Park, Ohio, 1985).
[2] J. Jaarinen, A. Lehto, and M. Luukala, *1983 Ultrasonic Symposium Proceedings*, edited by B. R. McAvoy (IEEE, New York, 1983), p. 659.
[3] G. Busse and H. G. Walther, in *Progress in Photoacoustic and Photothermal Sciences and Technology*, edited by A. Mandelis, Vol. 1 (Elsevier, New York, 1991), Chap. 5, p. 205.
[4] R. Riesen and H. Sommerauer, Am. Lab. (Fairfield, Conn.) **15**, No. 1, 30 (1983).
[5] M. Munidasa, M. T. Chi, A. Mandelis, S. K. Brown, and L. Mannik, Mat. Sci. Eng. A **159**, 111 (1992).

[6] L. Qian and P. Li, Appl. Opt. **29**, 4241 (1990).
[7] W. P. Leung and A. C. Tam, J. Appl. Phys. **56**, 153 (1984).
[8] S. B. Peralta, S. C. Ellis, C. Christofides, and A. Mandelis, J. Res. Non-Destruct. Eval. **3**, 69 (1991).
[9] Z. Chen and A. Mandelis, Phys. Rev. B **46**, 13 526 (1992).
[10] D. S. Day, M. T. Tsai, B. G. Streetman, and D. V. Lang, J. Appl. Phys. **50**, 5093 (1979).
[11] A. Rosencwaig and A. Gersho, J. Appl. Phys. **47**, 64 (1976).
[12] Model SR850 DSP lock-in amplifier manual (Stanford Research Systems, Inc., Sunnyvale, California, 1992).
[13] A. Mandelis and Z. Chen, Rev. Sci. Instrum. **63**, 2977 (1992).
[14] C. A. B. Ball and A. B. Conibear, Rev. Sci. Instrum. **62**, 2831 (1991).
[15] A. Mandelis (unpublished).
[16] A. Mandelis, in *Topics in Current Physics*, Vol. 47, edited by P. Hess (Springer, Heidelberg, 1990), Chap. 8.
[17] B. P. Lathi, *Communication Systems* (Wiley, New York, 1968), Chap. 2.7.